

PolyMAC: A Comparison

Staggered Finite Volume Methods on General Meshes

GdR MaNu, 24 Octobre 2023

P.-L. Bacq (pierre-loic.bacq@cea.fr), A. Gerschenfeld, M. Ndjinga

UNIVERSITÉ PARIS-SACLAY, CEA SACLAY

Outline

Introduction

PolyMAC

Test problems

Numerical Results

Comparisons

Numerical Resolution

Conclusions



Outline

Introduction

PolyMAC

Test problems

Numerical Results

Comparisons

Numerical Resolution

Conclusions





Motivation

- Development of codes for nuclear safety
- Challenging: conservation mass at the discrete level, treatment of spurious modes, precision at low Mach numbers,...
- MAC scheme does it all! Unfortunately, only on Cartesian meshes \Rightarrow limited in practice.

Objective: develop a generalization of the MAC scheme on the general meshes - called PolyMAC



PolyMAC

- PolyMAC: **family** of numerical schemes for multiphase compressible flows on **general** meshes (hexahedra, prisms, tetrahedra,...)
- Currently, three versions implemented in TRUST platform => PolyMAC I, II and III.
- Simplification: incompressible NS equations.



PolyMAC

- PolyMAC: **family** of numerical schemes for multiphase compressible flows on **general** meshes (hexahedra, prisms, tetrahedra,...)
- Currently, three versions implemented in TRUST platform => PolyMAC I, II and III.
- Simplification: incompressible NS equations.

Objectives:

- Description of the 3 schemes
- Definition of a benchmark (2D and 3D)
- Comparison: order of convergence, numerical computability
- Define guidelines for the user



General principle

PolyMAC: Finite Volume (FV) **generalization** of the MAC scheme to polyhedral meshes. The main unknowns are then:

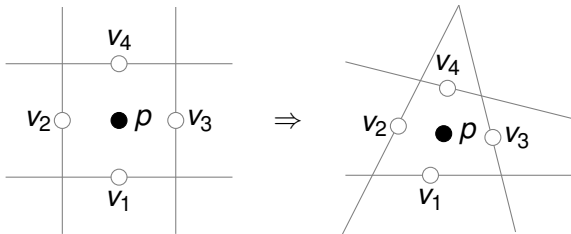
- normal component of the **velocity** at the **faces**
- **pressure** at the **cells**



General principle

PolyMAC: Finite Volume (FV) **generalization** of the MAC scheme to polyhedral meshes. The main unknowns are then:

- normal component of the **velocity** at the **faces**
- **pressure** at the **cells**





Incompressible Navier-Stokes equations

Find \vec{u} and p such that

$$\begin{aligned}\partial_t \vec{u} + (\vec{u} \cdot \nabla) \vec{u} - \nu \Delta \vec{u} + \nabla p &= \vec{f} \quad \text{in } \Omega, \\ \nabla \cdot \vec{u} &= 0 \quad \text{in } \Omega,\end{aligned}\tag{1}$$

- \vec{u} : fluid velocity
- p : pressure
- $\nu > 0$: viscosity
- $\Omega \subset \mathbb{R}^d$: unit square in 2D (unit cube in 3D)

Outline

Introduction

PolyMAC

Test problems

Numerical Results

Comparisons

Numerical Resolution

Conclusions





PolyMAC I

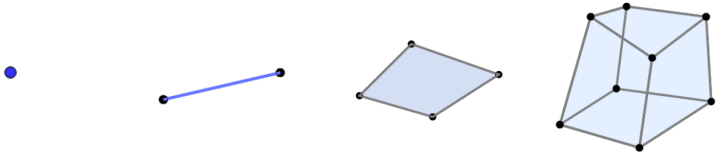
Reformulation of Equation (1) with the vorticity:

$$\begin{aligned} \text{Momentum:} \quad & \partial_t \vec{u} + \nabla \cdot (\vec{u} \otimes \vec{u}) + \nu \nabla \times \vec{\omega} + \nabla p = \vec{f}, \\ \text{Vorticity:} \quad & \nabla \times \vec{u} - \vec{\omega} = 0, \quad (2) \\ \text{Divergence:} \quad & \nabla \cdot \vec{u} = 0. \end{aligned}$$

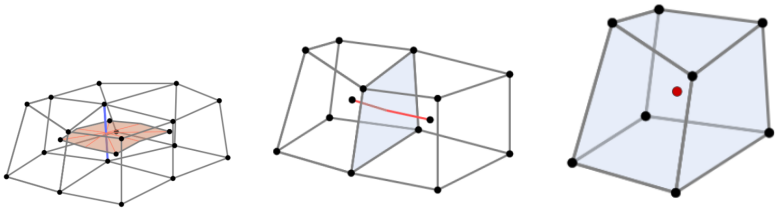
- Mimetic finite volumes (Bonelle (2014), Beltman (2018))
- Stability (star-shaped mesh) and discrete conservation law
- Introduction of a dual mesh



PolyMAC Control Volumes



(a) Primal Vertex s (b) Primal Edge a (c) Primal Face f (d) Primal Cell e



(a) Dual Edge \bar{a}

(b) Dual Face \bar{f}

(c) Dual Cell \bar{e}



Mimetic methods for PolyMAC

Use of **mimetic** methods:

- Control volumes chosen so that differential operators have **exact** representation based on integral theorems such as

$$\int_e \nabla \cdot \vec{v} = \int_{\partial e} \vec{v} \cdot \vec{n}_{\partial e}$$

In terms of discrete unknowns, if the divergence is discretized at the cells and the velocity at the faces:

$$[\nabla \cdot \vec{v}]_e = \frac{1}{|e|} \sum_{f \in e} |f| [v]_f = (D[v]_F)_e$$



Mimetic methods for PolyMAC

Use of **mimetic** methods:

- Control volumes chosen so that differential operators have **exact** representation based on integral theorems such as

$$\int_e \nabla \cdot \vec{v} = \int_{\partial e} \vec{v} \cdot \vec{n}_{\partial e}$$

In terms of discrete unknowns, if the divergence is discretized at the cells and the velocity at the faces:

$$[\nabla \cdot \vec{v}]_e = \frac{1}{|e|} \sum_{f \in e} |f| [v]_f = (D[v]_F)_e$$

- **Approximation** introduced to link primal to dual mesh
 - the primal edges A to the dual edges \bar{A} :

$$[\omega]_{\bar{A}} \approx (M^{(1)} [\omega]_A)$$

- the primal faces F to the dual faces \bar{F} :

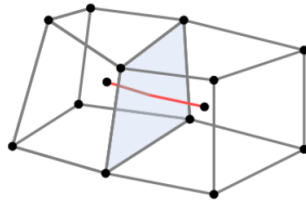
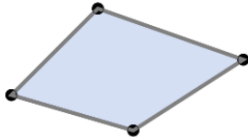
$$[v]_{\bar{F}} \approx (M^{(2)} [v]_F).$$



Choice of Control Volumes

For PolyMAC I, the control volumes are

- Velocity at the faces f and momentum at the dual faces \bar{f}
 - Time derivative $[\partial_t \vec{v}]_{\bar{F}} = M^{(2)} \partial_t [v]_F$
 - Vorticity curl $[\nu \nabla \times \vec{\omega}]_{\bar{F}} = M^{(2)} R^F [\omega]_A$
 - Pressure gradient $[\nabla p]_{\bar{F}} = G [p]_{\bar{E}}$

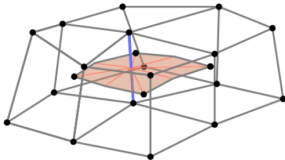




Choice of Control Volumes

For PolyMAC I, the control volumes are

- Velocity at the **faces** f and momentum at the **dual faces** \bar{f}
- Vorticity at the **edges** a and its definition at the **dual edges** \bar{a}
 - Velocity curl $[\nabla \times \vec{v}]_{\bar{A}} = R^A M^{(2)} [v]_F$
 - Vorticity $[\omega]_{\bar{A}} = M^{(1)} [\omega]_A$

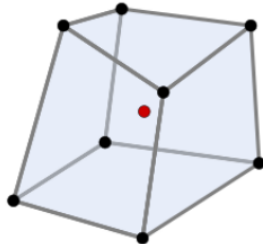
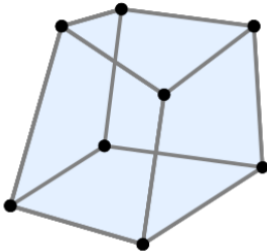




Choice of Control Volumes

For PolyMAC I, the control volumes are

- Velocity at the **faces** f and momentum at the **dual faces** \bar{f}
- Vorticity at the **edges** a and its definition at the **dual edges** \bar{a}
- Pressure at the **dual cells** \bar{e} and continuity at the **cells** e
 - Divergence $[\nabla \cdot \vec{v}]_E = D[v]_F$





PolyMAC I: Linear System

Resulting linear system:

$$\begin{pmatrix} \frac{M^{(2)}}{\Delta t} + C^F([v]_F^t) & M^{(2)} R^F & G \\ R^A M^{(2)} & -\frac{1}{\nu} M^{(1)} & 0 \\ -D & 0 & 0 \end{pmatrix} \begin{pmatrix} [v]_F^{t+\Delta t} \\ \nu [\omega]_A^{t+\Delta t} \\ [p]_{\bar{E}}^{t+\Delta t} \end{pmatrix} = \begin{pmatrix} \frac{M^{(2)}}{\Delta t} \mathbf{u}_f^t \\ 0 \\ 0 \end{pmatrix}, \quad (3)$$

- $C([v]_F^t)$: convection \Rightarrow NS linearised at each time step
- Without convection, symmetric matrix
- **Saddle-point** system
- $M^{(2)}$: not diagonally dominant on deformed meshes



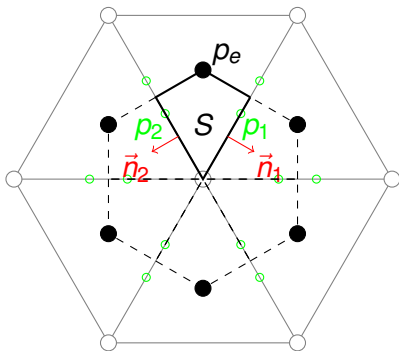
PolyMAC II

PolyMAC II: simplification of the top-left block and avoid saddle-point bottleneck.

- Discretization of the momentum equation at the **faces** f and the velocity at the **faces** f $[v]_f$
- Discretization of the continuity equation at the **cells** e and the pressure at the **dual cells** \bar{e} $[p]_{\bar{e}}$
- Convection and diffusion terms: complicated
⇒ auxiliary variables: velocity at the elements $[\vec{v}]_e$.
- Gradient: not an exact operator anymore
⇒ MPFA for the gradients (Aavatsmark 2002)



MPFA schemes



Approached the gradient in the cell e

$$\nabla p_e \leftarrow G(p) = \frac{1}{|S|} \left((p_1 - p_e) \vec{n}_1^T + (p_2 - p_e) \vec{n}_2^T \right), \quad (4)$$

Imposes continuity of the flux

$$\nabla p_e \cdot \vec{n}_2 + \nabla p_{e'} \cdot \vec{n}_2 = 0, \quad (5)$$



Discretization of the equations

Mass equation:

- As for PolyMAC I: $[\nabla \cdot \vec{v}]_E = (D[v]_F)$

Momentum equation:

- Time derivative: $[\partial_t \vec{v}]_f = (M_f \partial_t [v]_F)_f$
- Pressure gradient: use of the MPFA method $[\nabla \rho]_f = (G^{MPFA} [\rho]_{\bar{E}})_f$
- Diffusion term:
 - 1 Velocity at the cells $[\vec{v}]_e$ reconstructed from $[v]_f$
 - 2 MPFA used to compute $[\nu \nabla \vec{v}]_f$ and integral theorems yield

$$[\nabla \cdot (\nu \nabla \vec{v})]_e = \frac{1}{|e|} \sum_{f \in e} |f| [\nu \nabla \vec{v}]_f$$

- 3 Interpolate the term to the faces:

$$[\nabla \cdot (\nu \nabla \vec{v})]_f = \mu [\nabla \cdot (\nu \nabla \vec{v})]_e + (1 - \mu) [\nabla \cdot (\nu \nabla \vec{v})]_{e'}$$



Discretization of the equations (cont'd)

■ Convection term:

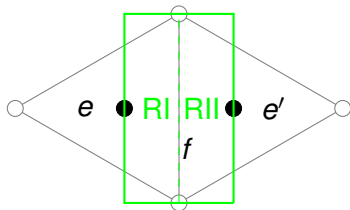
- 1 Velocity at the cells $[\vec{v}]_e$ reconstructed from $[v]_f$
- 2 Apply a convection term to the velocity

$$[\nabla \cdot (\vec{v} \otimes \vec{v})]_e = \frac{1}{|e|} \sum_{f \in e} |f| [v]_f [v]_{cv},$$

where $[v]_{cv}$ depends on the chosen convection scheme: upwind or centered.

- 3 Finally, the convection term is interpolated at the faces from the neighbouring cell values. The left element will contribute for the ratio $\mu = RII/(RI + RII)$ while the right element will contribute for the ratio $1 - \mu$:

$$[\nabla \cdot (\vec{v} \otimes \vec{v})]_f = \mu [\nabla \cdot (\vec{v} \otimes \vec{v})]_e \cdot \vec{n}_f + (1 - \mu) [\nabla \cdot (\vec{v} \otimes \vec{v})]_{e'} \cdot \vec{n}_f, \quad (6)$$





Linear system for PolyMAC II

Resulting linear system:

$$\begin{pmatrix} \frac{l}{\Delta t} & C_f(\mathbf{u}_c^t) + D_f(\mathbf{u}_c^t) & G_f^{MPFA} \\ 0 & \frac{l}{\Delta t} + C_c(\mathbf{u}_c^t) + D_c(\mathbf{u}_c^t) & G_c^{MPFA} \\ G^T & 0 & 0 \end{pmatrix} \begin{pmatrix} \mathbf{u}_f^{t+\Delta t} \\ \mathbf{u}_c^{t+\Delta t} \\ \mathbf{p}_c^{t+\Delta t} \end{pmatrix} = \begin{pmatrix} \frac{l}{\Delta t} \mathbf{u}_f^t \\ \frac{l}{\Delta t} \mathbf{u}_c^t \\ 0 \end{pmatrix} \quad (7)$$

- Saddle point manageable (l instead of M_u)
- High numerical cost on some meshes (tetrahedra,...)
- Not symmetric in the Stokes case



PolyMAC III

Best of both worlds: **simple top left block**, numerical cost **under control**.

- Same formulation as PolyMAC I:

$$\begin{aligned} \text{Momentum:} \quad & \partial_t \vec{u} + \nabla \cdot (\vec{u} \otimes \vec{u}) + \nu \nabla \times \vec{\omega} + \nabla p &= \vec{f}, \\ \text{Vorticity:} \quad & \nabla \times \vec{u} - \vec{\omega} &= 0, \\ \text{Divergence:} \quad & \nabla \cdot \vec{u} &= 0. \end{aligned} \quad (8)$$

- Except momentum at the faces:
 - Velocity at the **faces f** and momentum at the **faces f**
 - Vorticity at the **edges a** and its definition at the **dual edges \bar{a}**
 - Pressure at the **dual cells \bar{e}** and continuity at the **cells e**
- Convection similar to PolyMAC II
- Pressure gradient with HFV: auxiliary pressure at the faces



Resulting linear system

$$\begin{pmatrix} \frac{1}{\Delta t} + C^F([v]_F^t) & R^F & G_e^{HFV} & G_f^{HFV} \\ R^A M^{(2)} & -\frac{1}{\nu} M^{(1)} & 0 & 0 \\ -D & 0 & 0 & 0 \\ 0 & 0 & P_e & P_f \end{pmatrix} \begin{pmatrix} [v]_F^{t+\Delta t} \\ \nu [\omega]_A^{t+\Delta t} \\ [\rho]_{\bar{E}}^{t+\Delta t} \\ [\rho]_F^{t+\Delta t} \end{pmatrix} \quad (9)$$

$$= \begin{pmatrix} \frac{1}{\Delta t} [v]_F^t \\ 0 \\ 0 \\ 0 \end{pmatrix} \quad (10)$$

- Saddle point manageable (l instead of M_u)
- Numerical cost reasonable on all meshes
- Not symmetric for Stokes problems

Outline

Introduction

PolyMAC

Test problems

Numerical Results

Comparisons

Numerical Resolution

Conclusions





2D and 3D test problems

In 2D: Bercovier-Engelman test for a right-hand-side of the form:

$$\vec{f} = \begin{pmatrix} f_1(x, y) + (y - \frac{1}{2}) \\ -f_1(y, x) + (x - \frac{1}{2}) \end{pmatrix}, \quad (11)$$

where $f_1(x, y) =$

$$256[x^2(x-1)^2(12y-6) + y(y-1)(2y-1)(12x^2-12x+2)]$$

In 3D: rotating Navier-Stokes problem ($\nu = 10^{-2}$, $Re = 100$)

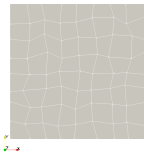
$$\vec{u} = \begin{pmatrix} y - z \\ z - x \\ x - y \end{pmatrix} \quad (12)$$

$$p = (x^2 + y^2 + z^2) - xy - xz - yz - \frac{1}{4}$$

(Extensively used in FVCA benchmarks)



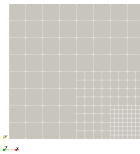
Meshes



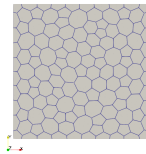
(a) Quadrangles



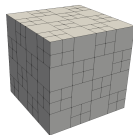
(b) Triangles



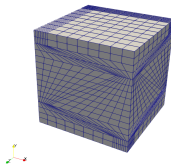
(c) Locally Refined



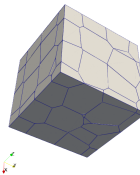
(d) Polygons



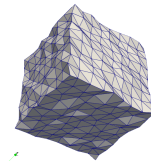
(e) Checkerboard



(f) Kershaw



(g) Voronoi



(h) Random

Figure 3: Representation of some meshes from the benchmark.

Outline

Introduction

PolyMAC

Test problems

Numerical Results

Comparisons

Numerical Resolution

Conclusions





Convergence (in velocity)

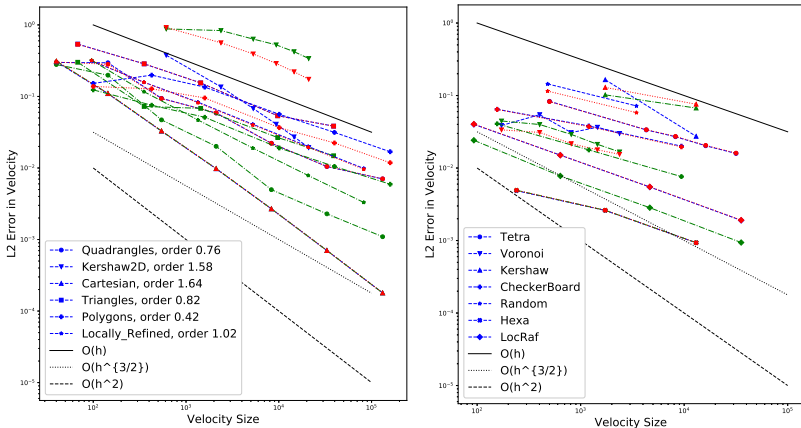


Figure 4: Left: 2D meshes; right: 3D meshes. PolyMAC I is represented in blue, PolyMAC II in green and PolyMAC III in red.



Convergence: 2D

PolyMAC	Velocity		
	I	II	III
Cartesian	1.64	1.66	1.66
Triangles	0.82	1.32	0.82
Quadrangles	0.76	1.06	0.78
Polygons	0.42	0.74	0.50
Locally Refined 2D	1.02	1.50	1.04
Kershaw 2D	1.58	0.44	0.86

Table 1: Estimated order of convergence for all three PolyMAC versions on the 2D meshes.



Convergence: 3D

PolyMAC	Velocity		
	I	II	III
Hexahedras	1.08	1.11	1.11
Locally Refined 3D	1.53	1.71	1.53
Kershaw 3D	2.67	0.63	0.78
Checker Board	0.84	1.23	0.84
Voronoi	0.36	1.02	0.90
Tetrahedras	1.23	/	1.20
Random	1.05	/	1.05

Table 2: Estimated order of convergence for all three PolyMAC versions on the 3D meshes.



Sparsity: 2D

PolyMAC	Sparsity Ratio		
	I	II	III
Cartesian	9.93	10.14	4.65
Triangles	8.92	27.23	7.95
Quadrangles	11.91	20.48	9.96
Polygons	18.13	18.42	14.12
Locally Refined 2D	9.95	10.16	4.68
Kershaw 2D	11.67	17.58	9.42

Table 3: Nnz per row on the 2D meshes.



Sparsity: 3D

PolyMAC	Sparsity Ratio		
	I	II	III
Hexahedras	19.61	12.86	6.94
Locally Refined 3D	23.24	13.93	8.34
Kershaw 3D	42.48	47.68	31.52
Checker Board	91.05	29.64	54.27
Voronoi	148.76	53.58	117.15
Tetrahedras	24.35	KO	20.29
Random	72.65	KO	63.53

Table 4: Nnz per row on the 3D meshes.

Outline

Introduction

PolyMAC

Test problems

Numerical Results

Comparisons

Numerical Resolution

Conclusions





Comparisons

PolyMAC	Accuracy	Computational cost	Stability
I	+	-	++
II	++	- -	(-)
III	+	++	(-)

(-) Sometimes divergent

- PolyMAC II most **accurate** BUT **heavy**
- PolyMAC III **as accurate** as PolyMAC I but **much sparser** ⇒ **Default option**
- PolyMAC I **always** convergent BUT **saddle point** ⇒ **Back-up option**

P.-L. Bacq, A. Gerschenfeld, M. Ndjinga, PolyMAC: Staggered Finite Volume Methods on General Meshes for Incompressible Navier-Stokes Problems, *FVCA X*, 2023.

Outline

Introduction

PolyMAC

Test problems

Numerical Results

Comparisons

Numerical Resolution

Conclusions





Towards industrial cases

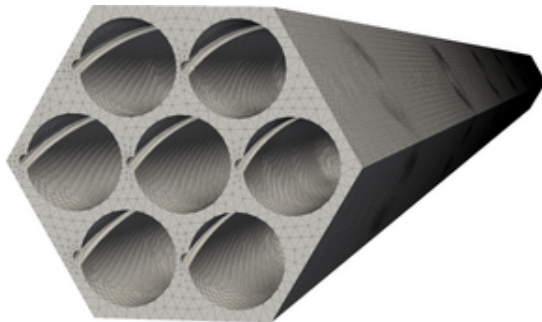


Figure 5: Sodium fast reactor Assembly mesh

- More complex than FVCA meshes
- Spacer => poor cells
- No satisfactory method without efficient linear solver



PolyMAC I system

$$\begin{pmatrix} \frac{M_u}{\Delta t} + C(\mathbf{u}_f^t) & R & G \\ R^T & -\frac{1}{\nu} M_\omega & 0 \\ G^T & 0 & 0 \end{pmatrix} \begin{pmatrix} \mathbf{u}_f^{t+\Delta t} \\ \nu \boldsymbol{\omega}_e^{t+\Delta t} \\ \mathbf{p}_c^{t+\Delta t} \end{pmatrix} = \begin{pmatrix} \frac{M_u}{\Delta t} \mathbf{u}_f^t \\ 0 \\ 0 \end{pmatrix}$$

- Double saddle point system
- Hard to solve with iterative methods
- Direct solvers restrict the size of the problem



Prediction-correction method

Currently, the solving step is implemented as a correction-prediction method:

- 1 Prediction: Momentum equation on its own to find first approximation of \vec{u}
- 2 Correction: Poisson equation on pressure to enforce $\nabla \cdot \vec{u} = 0$

Linear system for the prediction:

$$\begin{pmatrix} \frac{M_U}{\Delta t} + F & R_U \\ R_O & M_P \end{pmatrix} \begin{pmatrix} \mathbf{u}^* \\ \nu\omega \end{pmatrix} = \begin{pmatrix} \frac{M_U}{\Delta t} \mathbf{u}^t - B^T \mathbf{p} \\ \mathbf{p} \end{pmatrix} \quad (13)$$

Solved by GMRES preconditioned by a block ILU method *i.e.* both the velocity block and the Schur complement are preconditioned by ILU.



Prediction-correction method

Currently, the solving step is implemented as a correction-prediction method:

- 1 Prediction: Momentum equation on its own to find first approximation of \vec{u}
- 2 Correction: Poisson equation on pressure to enforce $\nabla \cdot \vec{u} = 0$

Linear system for the correction:

$$\begin{pmatrix} M_U & B^T \\ -B & 0 \end{pmatrix} \begin{pmatrix} \delta \mathbf{u} \\ \Delta t \delta \mathbf{p} \end{pmatrix} = \begin{pmatrix} \mathbf{0} \\ -B \mathbf{v}^* \end{pmatrix} \quad (13)$$

Solved by a **direct solver** \Rightarrow bottleneck of the approach.



Classical Approach for Saddle-Point problems

Block preconditioner for a Krylov subspace method:

$$\begin{pmatrix} M_U & \\ & S \end{pmatrix} \Rightarrow \begin{pmatrix} \tilde{M}_U & \\ & \tilde{S} \end{pmatrix} \quad (14)$$

- \tilde{M}_U : approximation of M_U
- \tilde{S} : approximation of $S = BM_U^{-1}B^T$ (typically: $BD_U^{-1}B^T$).



Classical Approach for Saddle-Point problems

Block preconditioner for a Krylov subspace method:

$$\begin{pmatrix} M_U & \\ & S \end{pmatrix} \Rightarrow \begin{pmatrix} \tilde{M}_U & \\ & \tilde{S} \end{pmatrix} \quad (14)$$

- \tilde{M}_U : approximation of M_U
- \tilde{S} : approximation of $S = BM_U^{-1}B^T$ (typically: $BD_U^{-1}B^T$).

Size	Iterations		
	Cartesian	Kershaw 2D	Assembly
1	8	66	NO
2	8	82	NO
3	8	93	NO
4	8	110	/
5	10	140	/
6	10	131	/



An algebraic transformation

Algebraic transformation of the system to give it a more suitable structure:

- Change of variables:

$$\begin{pmatrix} \mathbf{u} \\ \mathbf{p} \end{pmatrix} = \begin{pmatrix} I & -D_U^{-1} B^T \\ & I \end{pmatrix} \begin{pmatrix} \hat{\mathbf{u}} \\ \hat{\mathbf{p}} \end{pmatrix},$$

where D_U is the diagonal of M_U . The transformed system becomes:

$$\begin{pmatrix} M_U & (I - M_U D_U^{-1}) B^T \\ -B & B D_U^{-1} B^T \end{pmatrix}$$

Advantages:

- More weight on the diagonal blocks (easier for iterative methods)
- Pressure block has a Laplacian-like structure: $\hat{C} = B D_U^{-1} B^T$



Preconditioning the transformed system

Stokes-like system if reorder the transformed system ($\mathbf{u} \leftrightarrow \mathbf{p}$):

$$\begin{pmatrix} BD_U^{-1}B^T & -B \\ (I - M_U D_U^{-1})B^T & M_U \end{pmatrix}$$

State-of-the-art block preconditioner:

- $\hat{C} = BD_U^{-1}B^T$: similar to a discrete Laplacian \Rightarrow AMG preconditioner
- M_U : mass matrix *spectrally equivalent* to Schur complement $\Rightarrow 2M_U$

$$\begin{pmatrix} \tilde{C} & \\ & 2\tilde{M}_U \end{pmatrix}$$



Numerical Results

Size	Cartesian		Kershaw 2D		Assembly	
	Class.	Transf.	Class.	Transf.	Class.	Transf.
1	8	5	66	35	NO	88
2	8	4	82	42	NO	49
3	8	4	93	49	NO	25
4	8	4	110	54	/	/
5	10	4	140	56	/	/
6	10	4	131	55	/	/

Outline

Introduction

PolyMAC

Test problems

Numerical Results

Comparisons

Numerical Resolution

Conclusions





Conclusions

- General FV scheme for Navier-Stokes equations
- Implemented for compressible multi-phasic flows
- Key issue identified: iterative solver
- Robust iterative solver for Correction step \Rightarrow **full iterative process**
- Work in progress: Iterative solver for the full 3×3 system
- Implemented in PETSc

Thank you! Any questions?